

pubs.acs.org/Macromolecules Article

Controlling Morphological Transitions of Polymeric Nanoparticles via Doubly Responsive Block Copolymers

Jared I. Bowman, Cabell B. Eades, Joanna Korpanty, John B. Garrison, Georg M. Scheutz, Sofia L. Goodrich, Nathan C. Gianneschi,* and Brent S. Sumerlin*



Cite This: Macromolecules 2023, 56, 3316-3323



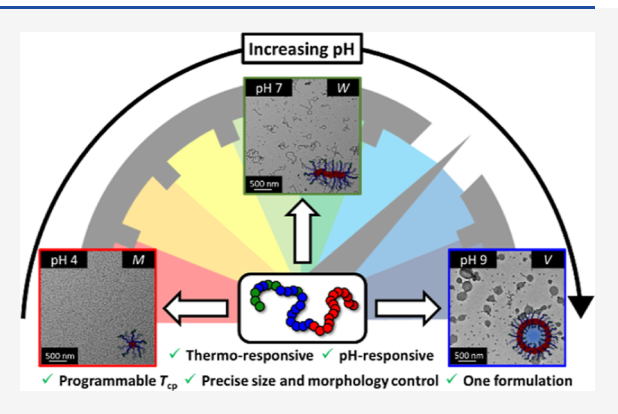
ACCESS I

III Metrics & More

Article Recommendations

s) Supporting Information

ABSTRACT: We report on a dual-responsive block copolymer system that exhibits a pH-dependent cloud point $(T_{\rm cp})$ and allows for precise control over the size and morphology of self-assembled nanostructures. By incorporating 2-(dimethylamino)ethyl methacrylate (DMAEMA), a pH- and temperature-responsive monomer, within the corona of a nanoparticle, the relative hydrophilic/hydrophobic block volumes can be controlled. Capitalizing on this phenomenon, we explore the temperature response of block copolymer assemblies at acidic, neutral, and basic pH, where the DMAEMA units are 99, 60, and 2% protonated. In general, as pH decreases, the corona was observed to swell due to charge repulsion and increased hydration, attenuating temperature sensitivity. By systematically varying the pH, temperature, and content of DMAEMA, we develop several systems that can readily form micelles, worms, and vesicles from a single block copolymer composition.



■ INTRODUCTION

Polymerization-induced self-assembly (PISA) has emerged as a powerful tool to prepare nanoparticles. During PISA, a solvophilic polymer is chain-extended with a monomer that generates a solvophobic block.^{1,2} This increase in solvophobicity drives microphase separation to form block copolymer micelles. As the core block continues to grow, the micelles undergo further order—order transitions to form worms, vesicles, and lamellae. $^{3-10}$ Generally, morphology during PISA can be dictated by simply varying the length of the core-forming block, allowing for the facile synthesis of a range of morphologies from a single precursor block. As each morphology exhibits distinctive functions and properties, recent advances in polymer self-assembly have been focused on the development of "smart" nanoparticles. 11-14 These nanoparticles incorporate a stimuli-responsive moiety, allowing for morphological transitions (e.g., micelle-to-worm or wormto-vesicle) to occur upon the introduction of stimuli.² A major advantage of these systems is the ability to obtain micelles, worms, and vesicles from a single block copolymer formulation, allowing for the direct comparison of structureproperty relationships among chemically equivalent copolymers.15

The final morphology of block copolymers is dictated by an equilibrium between core-chain stretching, coronal chain repulsion, and interfacial tension. This delicate interplay determines the relative volume ratios of both the solvophilic and solvophobic blocks, which, in turn, determine the

morphology of the nanoparticles. In general, as the relative solvophobic block volume increases, the block copolymers undergo transitions to higher-order morphologies, such as worms or vesicles. As a consequence of the dynamic nature of block copolymer self-assembly, much interest has been generated in tuning morphological transitions of assemblies as a function of stimuli. Many strategies have been developed in the last decade to induce morphological transitions of micelles to worms or worms to vesicles via changes in pH, 17 temperature, ^{23–28} or light. ^{29–31} While the stimuli may vary in each of these methods, morphological transitions are all achieved by either altering the solvophilic or solvophobic block volumes. 13,15 As the morphology is dictated by relative volume fractions, the locus of the stimuli-responsive moiety along the chain can have significant implications on morphological transitions. For example, by investigating the behavior of compositionally distinct (diblock, gradient, asymmetric diblock, and triblock) copolymers, Harrison and co-workers found that diblock copolymers formed kinetically trapped assemblies, whereas compositionally heterogeneous copolymers could undergo dynamic morphological transitions in

Received: March 10, 2023 Revised: April 13, 2023 Published: April 28, 2023





response to pH.¹⁸ These results suggest that subtle manipulation of stimuli-responsive trigger placement gives rise to profound consequences on final block copolymer morphology.

Herein, we develop block copolymer systems with a pH-dependent cloud point $(T_{\rm cp})$, allowing for precise control over nanoparticle size and morphology. Temperature response increases with the increase in pH, allowing for the preparation of micelles, worms, and vesicles at concentrations as low as 0.1% w/w from a single formulation. This result is achieved by incorporating 2-(dimethylamino)ethyl methacrylate (DMAE-MA), a pH- and temperature-responsive monomer, within the corona of the nanoparticle. As DMAEMA contains a tertiary amine (p $K_a = 7.3$), at a pH below the p K_a , the hydrophilic block volume increases due to charge repulsion among DMAEMA moieties as well as increased hydration. In other words, as pH decreases, the hydrophilic block volume increases, favoring lower-order morphologies (Figure 1). This

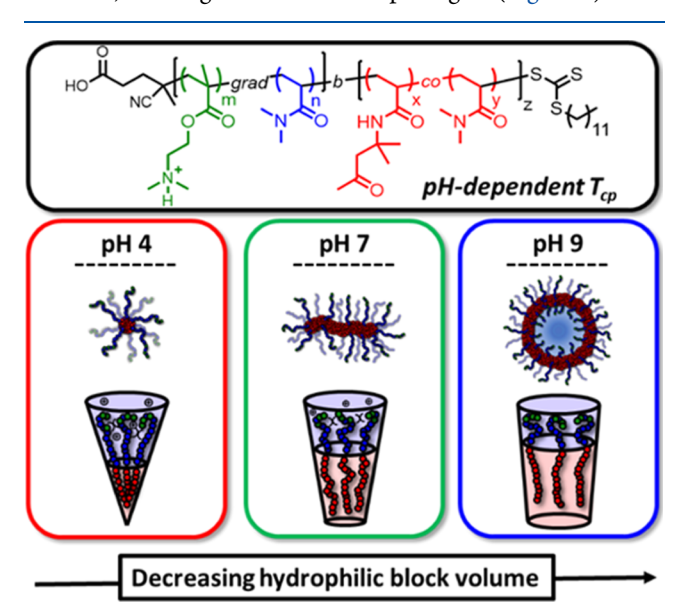


Figure 1. Size and morphology can be modulated by manipulating the hydrophilic block volume while maintaining a constant hydrophobic block volume. At low pH, the corona is increasingly swollen due to increased charge repulsion and hydration. This affords suppression of the cloud point temperature $(T_{\rm cp})$, leading to thermally stable nanoparticles. As the pH increases, the hydrophilic corona shrinks relative to the hydrophobic core, driving morphological evolution. This decrease in coronal hydration with pH results in increasingly temperature-responsive nanostructures.

increase in hydration causes the $T_{\rm cp}$ to increase, allowing for programming of temperature response. To achieve this, a series of macro chain-transfer agents (macroCTAs) containing varying mol % DMAEMA was synthesized and subsequently chain-extended to yield nanoparticles with DMAEMA-rich regions near the periphery of the corona. We show that systematic variation of the hydrophilic-to-hydrophobic volume ratios can be achieved by modulating the core-chain length, pH, temperature, and amount of DMAEMA, providing unprecedented control over both nanoparticle size and morphology. Utilizing these variables, we develop a straightforward method to form micelles, worms, or vesicles from a block copolymer by varying pH and temperature.

RESULTS AND DISCUSSION

We first synthesized a series of macroCTA copolymers containing varying amounts of DMAEMA (Figures 1 and 2) to control the degree of stimuli-response, with the polymers containing more DMAEMA hypothesized to exhibit a greater response. Specifically, we copolymerized 10, 20, and 30 mol % of DMAEMA with N_iN_i -dimethylacrylamide (DMA) via reversible addition—fragmentation chain-transfer (RAFT) polymerization (Figure 2A). The pseudo-first-order kinetic plot (Figure 2B) revealed faster polymerization of DMAEMA, as expected for the disparate reactivity of methacrylates compared to acrylamides. The macroCTAs formed should be DMAEMA-rich at the α -end due to the higher reactivity and lower tendency of methacrylates to cross-propagate compared to acrylamides. 32

The polymerizations deviated from ideal behavior and rather followed a kinetic profile and an evolution of molecular weight with conversion typical for slow initiation (Figure 2B,C). We rationalize this may be due to the R-group of the CTA being better matched with methacrylates than acrylamides, leading to slow initialization because of the more stable methacrylatecentered radical. However, gel permeation chromatography (GPC) characterization revealed well-controlled macroCTAs of comparable sizes (Table S1) with good agreement between theoretical and experimental molecular weights (Table S1). Molar compositions of DMAEMA were determined via ¹H NMR spectroscopy by comparing the methylene signal next to the trithiocarbonate (δ = 3.40 ppm) to the signal of the methylene adjacent to the oxygen in DMAEMA (δ = 4.15 ppm) and the dimethyl signal in DMA ($\delta = 2.97$ ppm) (Figures S1-S3). With this approach, it was determined that the copolymers contained 12, 24, and 34 mol % DMAEMA, respectively.

With macroCTAs in hand, we set about performing PISA across several hydrophobic block degrees of polymerization (DPs; Figure 3). Since we sought to probe pH and temperature independently, the introduction of any thermal history into the assembly process was avoided by choosing photoinduced electron/energy transfer (PET) RAFT polymerization at room temperature. MacroCTAs were chain-extended with 30 mol % DMA and 70 mol % diacetone acrylamide (DAAm) via PET-RAFT PISA (10% w/w) to afford a library of nanoparticles across four hydrophobic DPs: 100, 150, 200, and 300 (Figure 3A). Copolymerization of DAAm and DMA during PISA has been previously reported to have dramatic effects on the solvation of the core. While higher molar amounts (90%) of DAAm result in kinetically trapped lowerorder assemblies, lower molar amounts (75 mol %) result in sufficient dynamicity to yield higher-order morphologies. With this in mind, we elected to use 70 mol % DAAm to further facilitate morphological transitions. Additionally, the use of DAAm as a core-forming monomer is well-reported in literature and conveniently provides a functional handle to allow for core-crosslinking of nanoparticles for transmission electron microscopy (TEM) analysis, ensuring capture of the actual morphology in solution regardless of sample preparation. 7,10,36 ¹H NMR spectroscopy revealed near-quantitative monomer conversion (>99%), as well as kinetics consistent with self-assembly, with the rate of monomer consumption increasing as micelle formation begins (Figure 3B). 3,35,34,36 Additionally, GPC analysis revealed monomodal peaks with clean molecular weight shifts to lower elution times (Figure

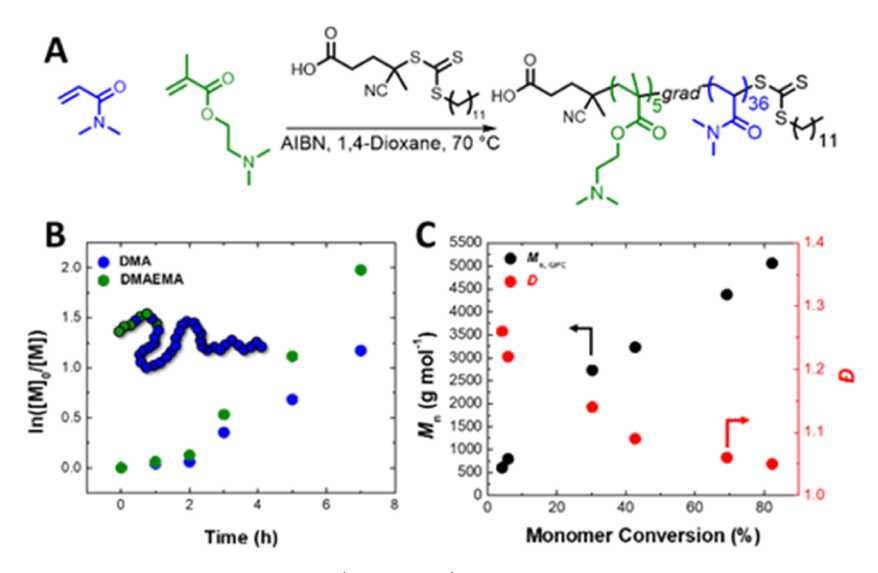


Figure 2. (A) Reaction scheme of macro chain-transfer agent (macroCTA) synthesis via reversible addition—fragmentation chain-transfer (RAFT) polymerization targeting $M_n = 5$ kDa; (B) the pseudo-first-order kinetic plot revealed a faster consumption of 2-(dimethylamino)ethyl methacrylate (DMAEMA) compared to N_i -dimethylacrylamide (DMA), indicative of a gradient composition; (C) number average molecular weight (M_n) and dispersity (D) vs conversion plot.

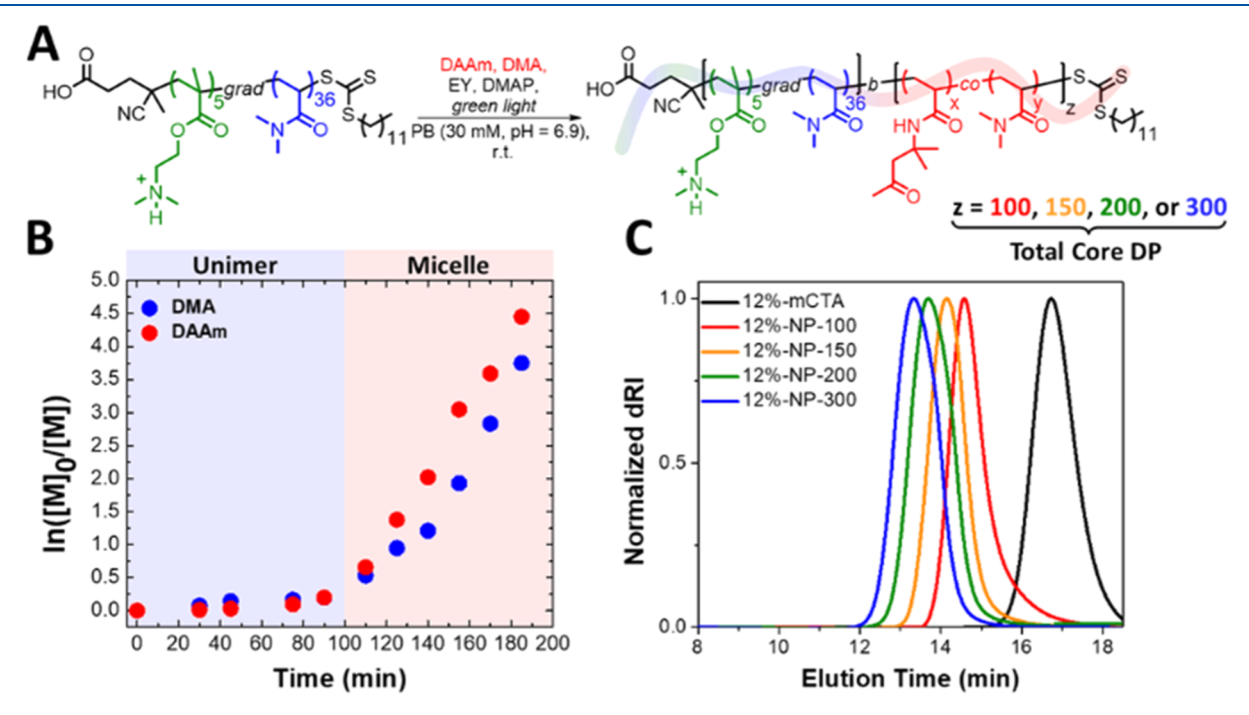


Figure 3. (A) Nanoparticle synthesis via photoinduced electron/energy transfer (PET) RAFT; (B) pseudo-first-order kinetic plot of the polymerization targeting $DP_{DMA-co-DAAm} = 100$ exhibited kinetic behavior consistent with self-assembly, with the rate of monomer consumption increasing upon micelle formation (100 min); and (C) gel permeation chromatography (GPC) trace revealed a clean shift in molecular weight upon chain-extension of macroCTA (black).

3C), as well as comparable molecular weights across each corechain length (Table S2). The assemblies were then diluted to 0.1% w/w and studied via variable-temperature dynamic light scattering (VT-DLS) to determine the change in hydrodynamic size as a function of temperature.

We first investigated the effect of core-chain length on temperature-induced morphological transitions; 0.1% w/w solutions of nanoparticles formed by mCTA-12% (12%-NP-100, 12%-NP-150, 12%-NP-200, and 12%-NP-300, where 12% refers to the amount of DMAEMA within the corona and 100, 150, 200, and 300 refer to the DP of the hydrophobic block)

were subjected to VT-DLS with a temperature range from 10–70 °C and a heating rate of 1 °C/min (Figure 4). When cooled to 10 °C, nanoparticles were roughly uniform in size (20–30 nm), with size slightly increasing as a function of core-chain length. However, upon heating, the implications of core-chain length became apparent, as nanoparticles containing longer hydrophobic blocks grew in size more rapidly than nanoparticles with shorter core-chain lengths. We found that large size changes can be accessed at lower temperatures in assemblies with longer core-chain length. For example, 12%-NP-300 (Figure 4, blue) showed a large size change between

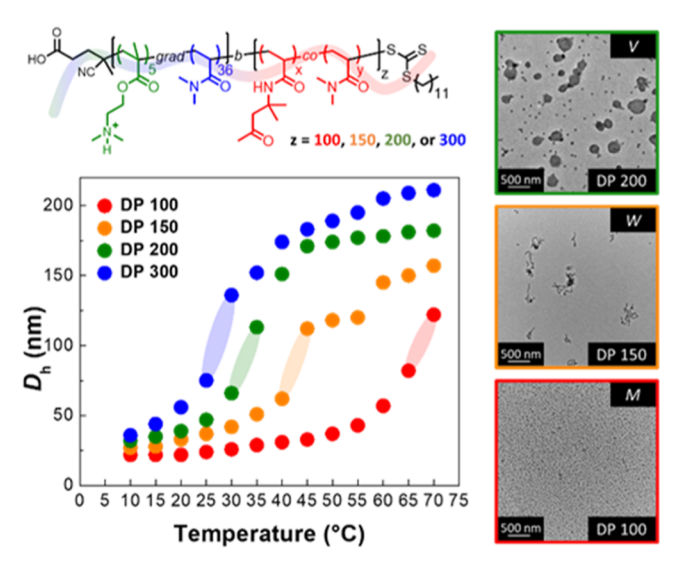


Figure 4. Investigation of morphological change as a function of corechain length revealed that polymers with shorter core-chain lengths exhibited a lower degree of temperature response compared to longer core-chain lengths (70% diacetone acrylamide). Heating 0.1% w/w solutions of nanoparticles to 50 °C (1 °C/min) yielded micelles (12%-NP-100, red), worms (12%-NP-150, orange), and vesicles (12%-NP-200, green).

25 and 30 °C, whereas 12%-NP-150 (Figure 4, orange) exhibited a similarly large size change between 40 and 45 °C. In general, the temperature response of this system can be tuned by varying the block copolymer length. In particular, 12%-NP-100 (Figure 4, red) exhibited no temperature response from 10 to 20 °C, remaining constant at 22 nm. From 25 to 50 °C, 12%-NP-100 displayed a linear size increase of about 0.4 nm/°C up to 37 nm, after which growth became exponential up to 122 nm at 70 °C. In contrast, 12%-NP-300 immediately exhibited a linear increase in size of 10 nm from 10-20 °C, increasing from 31 to 53 nm. Growth after 20 °C became exponential, doubling in size from 75 nm at 25 °C to 152 nm at 35 °C. Past 35 °C, 12%-NP-300 continued to grow at about 4 nm/°C, after which size began to plateau at 210 nm. It is important to note that although DLS demonstrates that the sizes of assemblies are temperature-dependent, these data are not necessarily indicative of a morphological transition. While the hydrodynamic sizes determined by DLS are contingent on the sphericity of the nanoparticles being characterized, the VT-DLS data in Figure 4 demonstrate that the assemblies are temperature-dependent and that the thermal response is dependent on the length of the core-chain.

To gain more accurate insights into morphological evolution, we analyzed nanoparticles via TEM. We chose to analyze the nanoparticle solutions at 50 °C to demonstrate the difference in temperature response and morphology, as the nanoparticle size difference between core-chain lengths is greatest at this temperature. To preserve the morphology of assemblies during dry-state analysis, *O*-alkyl hydroxylamine crosslinker was added to core-crosslink the assemblies via oxime formation. Nanoparticle solutions (0.1% w/w) were heated to 50 °C, after which 10 mol % crosslinker (with respect to DAAm) was added, and the solutions were allowed to react overnight at 50 °C. Upon cooling, the size of the assemblies remained the same (Figure S11), indicating successful core crosslinking. Imaging via TEM revealed that different morphologies could be accessed by varying the length

of the core-forming block. More specifically, we found that at 50 °C, micelles, worms, or vesicles could be obtained by simply varying the core-chain DP from 100, 150, or 200, respectively (Figure 4).

We next sought to obtain a wide range of morphologies from a single formulation. To achieve this, we set about investigating temperature response as a function of pH. By varying the extent of DMAEMA protonation, we reasoned that the hydrophilic block volume could be readily controlled as both a function of increased coronal charge repulsion as well as increased hydration of the hydrophilic volume. To determine the effect of the extent of protonation on temperature response, a PDMAEMA homopolymer was synthesized via RAFT polymerization as a model compound (Figures S12 and S13). The homopolymer was then dissolved in 30 mM phosphate buffer at 0.1% w/w, and the solutions were titrated with either 1 M HCl or 1 M NaOH to pH 4.15, 6.91, or 8.98. Using the Henderson-Hasselbalch equation, it was estimated that PDMAEMA is 99.9, 60.7, and 2.1% protonated at pH 4.15, 6.91, and 8.98, respectively. Cloud point temperatures were determined by heating the samples from room temperature to 95 °C and referencing the temperature of the samples at 50% scattering intensity. It was found that $T_{\rm cp}$ increased as a function of protonation. At pH 8.98, PDMAEMA exhibited a T_{cp} at 34 °C, whereas decreasing the pH to 6.91 increased the T_{cp} of PDMAEMA to 68 °C (Figure S14). At pH 4.15, no thermal response was observed. The pH dependence of the $T_{\rm cp}$ in PDMAEMA can be rationalized by protonation of the tertiary amine moiety. At a lower pH, PDMAEMA experienced a greater degree of protonation, wherein the polymer became more hydrophilic and experienced greater polymer-solvent interactions. As pH increased, there was a lesser extent of protonation, decreasing the hydration of the DMAEMA units and allowing the T_{cp} to be accessed. We hypothesized that the pH-dependent cloud point could be leveraged to modulate the nanoparticle size by tuning the relative volume of the hydrophilic block.

With this in mind, nanoparticle solutions of 12%-NP-100 were prepared at 0.1% w/w and titrated with either 1 M HCl or 1 M NaOH to evaluate temperature response at pH 4.15 and pH 8.98, respectively (Figure 5). At 10 °C, we found that nanoparticles were nearly uniform in size (20-25 nm), regardless of pH. From 10 to 45 °C, we observed linear size growth at all pHs as nanoparticles at higher pHs grew slightly faster. Between 45 and 70 °C, the nanoparticles at pH 8.98 began to grow more rapidly, increasing in size linearly from 60 to 153 nm at 4 nm/°C. The assemblies at pH 6.91 began to experience a size increase around 60 °C, increasing in size from 57 to 122 nm. In contrast, the assemblies at pH 4.15 only exhibited a small, linear increase (Figure 5). By DLS, the greatest size disparity of nanoparticles between pHs was found to be at 65 °C, where the sizes were 44, 82, and 134 nm at pH 4.15, pH 6.91, and pH 8.98, respectively. To verify the utility of tuning temperature response with pH, we analyzed the morphology of nanoparticles via TEM. Nanoparticle solutions at each pH were subsequently heated to 65 °C, crosslinked, and imaged via TEM. It was found that by utilizing 12%-NP-100 at pH 4.15, pH 6.91, and pH 8.98, we could achieve micelles (Figure 5, red), worms (Figure 5, green), and vesicles (Figure 5, blue), respectively—all from a single block copolymer composition.

We next elected to consider the role of core-chain DP on stimuli-responsive morphological evolution. To this end, we

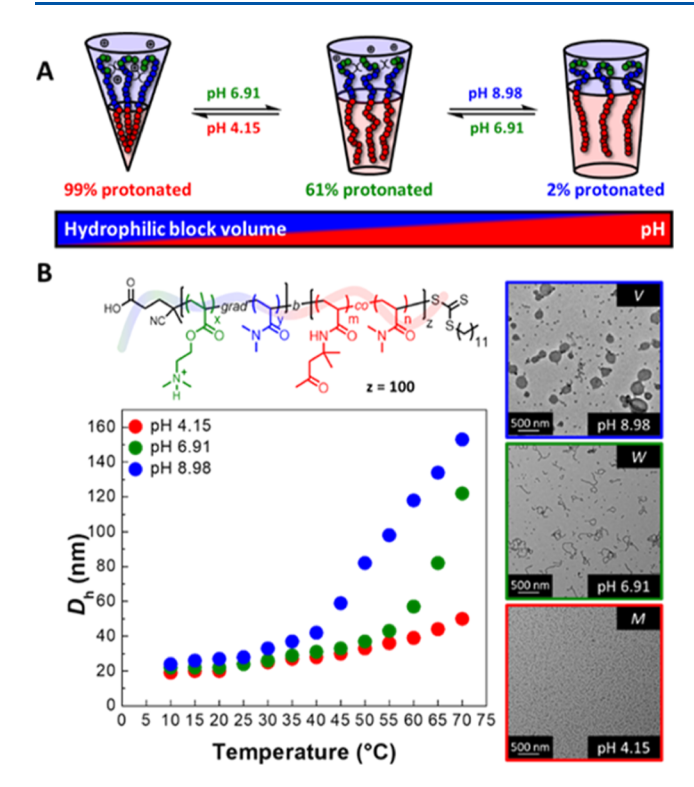


Figure 5. (A) Increasing pH causes the hydrophilic block volume to shrink relative to the hydrophobic block volume due to a lower degree of protonation. (B) At low pH, DMAEMA is increasingly protonated, suppressing temperature response (red). As pH increases, the cloud point temperature ($T_{\rm cp}$) becomes more readily accessed, allowing size growth at lower temperatures. By varying pH, micelles (red), worms (green), and vesicles (blue) can be obtained at 65 °C from a single block copolymer by varying pH.

prepared solutions of 12%-NP-100, 12%-NP-150, 12%-NP-200, and 12%-NP-300 at 0.1% w/w at the appropriate pH. We first analyzed assembly size as a function of pH at 25 $^{\circ}$ C (Table 1).

Table 1. Hydrodynamic Diameters (D_h) of Nanoparticle Solutions (0.1% w/w) at 25 °C and 70 °C across Varying pHs

sample	T (°C)	D _h (nm) ^a pH 4.15	D _h (nm) ^a pH 6.91	D _h (nm) ^a pH 8.98
12%-NP-100	25	24	23	28
12%-NP-150	25	27	34	44
12%-NP-200	25	31	43	59
12%-NP-300	25	35	92	95
12%-NP-100	70	48	122	158
12%-NP-150	70	55	145	221
12%-NP-200	70	63	182	264
12%-NP-300	70	76	205	325

^aAverage hydrodynamic diameter (D_h) was determined by DLS (0.1% w/w). Size distributions were averaged over five runs.

In general, size increased as a function of core-chain length and decreased as a function of increasing protonation. This is consistent with our earlier findings, wherein increasing protonation increased the hydrophilic block volume. At pH 4.15, nanoparticle size was similar (24–35 nm), whereas pH 6.91 and pH 8.98 exhibit similar size profiles. At 70 °C, however, this similarity disappeared, as the assemblies in pH

8.98 solution experienced a much greater size increase with sizes ranging from 158–325 nm (Table 1). Nanoparticles in pH 4.15 solution remained relatively small, ranging from 48 to 76 nm. These studies suggest that further modulation of size and morphology can be achieved by controlling the hydrophobic block volume as a function of core-chain length and varying the hydrophilic block volume via pH and temperature.

While our previous studies focused on block copolymers containing 12% DMAEMA, we reasoned that temperature and pH response could be accentuated by further increasing the DMAEMA content within the corona. Our initial investigation focused on block copolymers with a constant core-chain DP of 100, varying only the amount of DMAEMA within the corona. Block copolymer solutions were diluted to 0.1% w/w, titrated to the appropriate pH, and subjected to VT-DLS. At pH 4.15, assembly size decreased with the increase in DMAEMA content. Upon heating, each assembly exhibited a near-linear increase in size, with nanoparticles doubling in size for each block copolymer from 10 to 70 °C (Figure 6A). In general, the nanoparticles with a greater DMAEMA content were more protonated, and, therefore, displayed a larger hydrophilic block volume. This resulted in 24%-NP-100 and 34%-NP-100 being smaller and more thermally stable as they experience a larger degree of protonation.

As pH increased to 6.91, the same trend in size increase was observed, as the copolymers containing more DMAEMA were increasingly protonated. From 10 to 50 $^{\circ}\text{C}$, the size increase was linear for all block copolymers, after which the growth behavior deviated for each (Figure 6B). As 34%-NP-100 was the most protonated of the three copolymers, it displayed the least amount of size change, as it grew from 21 nm at 10 °C and plateaued at 36 nm by 50 °C. As the DMAEMA content decreased, 24%-NP-100 exhibited a mostly linear increase in size from 20 nm at 10 °C to 57 nm at 70 °C. Similarly, 12%-NP-100 grew linearly until 50 °C but then experienced exponential growth from 37 nm at 50 °C to 122 nm at 70 °C. At both pH 4.15 and 6.91, the solution was below the p K_a of DMAEMA (p $K_a = 7.3$); therefore, the coronas of each block copolymer were 99 and 61% protonated, respectively. As polymers containing more DMAEMA were more protonated, the thermal response was increasingly dampened as a function of pH. Conversely, once the pH of the solution was raised above the pK_a of DMAEMA, the opposite trend was observed, with polymers containing more DMAEMA experiencing a greater increase in size with temperature (Figure 6C). All formulations exhibited a slight linear growth (0.5 nm/°C) from 10-30 °C, after which a much greater linear growth was observed. This linear increase varied with DMAEMA content, with 12%-NP-100, 24%-NP-100, and 34%-NP-100 experiencing growth rates of 3.2, 3.6, and 4.1 nm/°C, respectively. These data suggest that the extent of stimuli response can be amplified by increasing DMAEMA content and that precise size control can be achieved by judicious pH and temperature control.

Finally, we applied these principles to block copolymers with longer core-chain lengths. Nanoparticle solutions were prepared in the same manner as previous studies; however, the size was investigated statically at 25 (Table S3) and 70 °C (Table S4). Corroborating previous data, the size increased with the increase in core-chain length. For pH 4.15 and pH 6.91 at 25 °C, the size decreased as a function of increasing DMAEMA content, as polymers with more DMAEMA exhibit a greater hydrophilic block volume. Conversely, once the pH

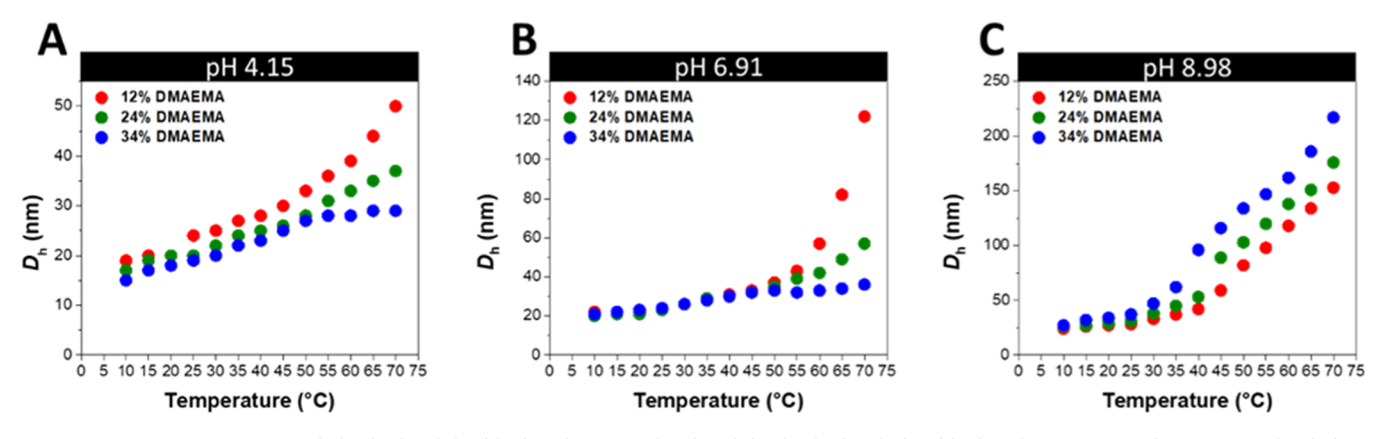


Figure 6. Increasing pH caused the hydrophilic block volume to shrink, while the hydrophobic block volume remained constant. This led to increasing temperature response with the increase in pH such that (A) at pH 4.15, the thermal response was largely suppressed due to increased hydration of the corona; (B) at pH 6.91, the thermal response was linear until 50 °C, after which the thermal response became exponential, linear, or plateaus with the increase in DMAEMA content; and (C) at pH 8.98, DMAEMA was largely deprotonated; therefore, the polymers with the most DMAEMA content exhibited the largest temperature response.

was above the p K_a , the size increased as a function of increasing DMAEMA content. Temperature response increased at higher pH, with each assembly roughly doubling in size from 25 to 70 °C at pH 4.15. At pH 6.91, temperature response became largely dependent on the amount of DMAEMA within the corona with 12%-NP-100–300 experiencing much larger growth than 34%-NP-100–300. As the DMAEMA content increased, assemblies began to become thermally unstable as macroscopic precipitation was observed at higher core-chain lengths (Table S4).

As pH 6.91 and pH 8.98 demonstrated the greatest temperature response, 12%-NP-200, 24%-NP-200, and 34%-NP-200 were imaged via TEM at 25 and 70 °C (Figure 7). At 25 °C and pH 6.91, only micelles were observed, regardless of the DMAEMA content. 12%-NP-200 underwent either a micelle-to-worm transition upon titration to pH 8.98 or a micelle-to-vesicle transition upon heating to 70 °C. When titrated from pH 6.91 to 8.98 or heated from 25 to 70 °C, 24%-NP-200 exhibited a micelle-to-worm transition. As 34%-NP-200 is more pH-sensitive, a micelle-to-vesicle transition was observed upon pH increase, whereas a micelle-to-worm transition was observed with the increase in temperature. From these images, we highlight that not only can micelles, worms, or vesicles be obtained from a single formulation but these transitions can also be obtained via pH or heat orthogonally.

CONCLUSIONS

By carefully modulating the pH and temperature of dualresponsive nanoparticles, it is possible to precisely control the nanostructure size and shape. The incorporation of DMAEMA in the corona provides a means to regulate the relative volume of the hydrophilic block through pH control. When the pH is lower than that of the pK_a of DMAEMA, the tertiary amine groups become protonated, causing the hydrophilic block to swell due to charge repulsion and increased hydration. Consequently, this protonation can be used to modulate the temperature sensitivity of the nanoparticles, allowing for a range of morphologies to be obtained from a single block copolymer composition. Furthermore, the DMAEMA content in the corona can be modified to control the nanoparticle shape. Importantly, this strategy circumvents the need for tedious nanoparticle synthesis by providing a straightforward means to prepare micelles, worms, and vesicles from a single

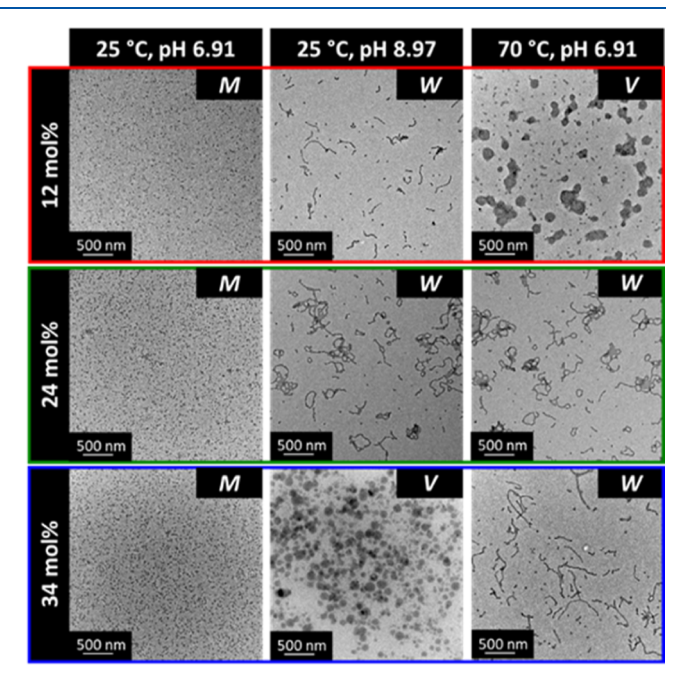


Figure 7. Although all block copolymers were micelles in pH 6.91 solution at 25 $^{\circ}$ C, each copolymer system displayed a unique behavior when subjected to pH or heat. At pH 8.97, copolymers with greater DMAEMA content experienced a larger pH response. At 70 $^{\circ}$ C in pH 6.91 solution, however, copolymers were \sim 60% protonated, allowing for increased temperature response with the decrease in DMAEMA content. Utilizing these stimuli orthogonally, 12%-NP-200 and 34%-NP-200 could form micelles, worms, or vesicles.

composition. This work demonstrates the potential of programmable block copolymers for the preparation of precisely defined nanoparticles, such as in drug delivery where both size and shape are critical design considerations.

ASSOCIATED CONTENT

Supporting Information

The Supporting Information is available free of charge at https://pubs.acs.org/doi/10.1021/acs.macromol.3c00445.

Materials and instrumentation, ¹H NMR spectra, GPC chromatographs, summary of GPC data, DLS traces, cloud point studies, and summary of DLS data (PDF)

AUTHOR INFORMATION

Corresponding Authors

Nathan C. Gianneschi — Department of Chemistry,
Northwestern University, Evanston, Illinois 60208, United
States; International Institute for Nanotechnology, Simpson
Querrey Institute, Chemistry of Life Processes Institute, Lurie
Cancer Center and Department of Materials Science &
Engineering, Department of Biomedical Engineering,
Department of Pharmacology, Northwestern University,
Evanston, Illinois 60208, United States; orcid.org/00000001-9945-5475; Email: nathan.gianneschi@
northwestern.edu

Brent S. Sumerlin — George & Josephine Butler Polymer Research Laboratory, Center for Macromolecular Science & Engineering, Department of Chemistry, University of Florida, Gainesville, Florida 32611, United States; orcid.org/ 0000-0001-5749-5444; Email: sumerlin@chem.ufl.edu

Authors

- Jared I. Bowman George & Josephine Butler Polymer Research Laboratory, Center for Macromolecular Science & Engineering, Department of Chemistry, University of Florida, Gainesville, Florida 32611, United States; ⊚ orcid.org/ 0000-0001-6469-2251
- Cabell B. Eades George & Josephine Butler Polymer Research Laboratory, Center for Macromolecular Science & Engineering, Department of Chemistry, University of Florida, Gainesville, Florida 32611, United States
- Joanna Korpanty Department of Chemistry, Northwestern University, Evanston, Illinois 60208, United States;
 occid.org/0000-0002-9274-5936
- John B. Garrison George & Josephine Butler Polymer Research Laboratory, Center for Macromolecular Science & Engineering, Department of Chemistry, University of Florida, Gainesville, Florida 32611, United States
- Georg M. Scheutz George & Josephine Butler Polymer Research Laboratory, Center for Macromolecular Science & Engineering, Department of Chemistry, University of Florida, Gainesville, Florida 32611, United States; orcid.org/ 0000-0001-5872-4333
- Sofia L. Goodrich George & Josephine Butler Polymer Research Laboratory, Center for Macromolecular Science & Engineering, Department of Chemistry, University of Florida, Gainesville, Florida 32611, United States

Complete contact information is available at: https://pubs.acs.org/10.1021/acs.macromol.3c00445

Notes

The authors declare no competing financial interest.

ACKNOWLEDGMENTS

This material was based on work supposed by the National Science Foundation (DMR-1904631) and DoD through the ARO (W911NF-17-1-0326).

REFERENCES

- (1) Penfold, N. J. W.; Yeow, J.; Boyer, C.; Armes, S. P. Emerging Trends in Polymerization-Induced Self-Assembly. *ACS Macro Lett.* **2019**, *8*, 1029–1054.
- (2) Pei, Y.; Lowe, A. B.; Roth, P. J. Stimulus-Responsive Nanoparticles and Associated (Reversible) Polymorphism via Polymerization Induced Self-Assembly (PISA). *Macromol. Rapid Commun.* **2017**, 38, 1600528.

- (3) Warren, N. J.; Armes, S. P. Polymerization-Induced Self-Assembly of Block Copolymer Nano-Objects via RAFT Aqueous Dispersion Polymerization. *J. Am. Chem. Soc.* **2014**, *136*, 10174–10185.
- (4) Canning, S. L.; Smith, G. N.; Armes, S. P. A Critical Appraisal of RAFT-Mediated Polymerization-Induced Self-Assembly. *Macromolecules* **2016**, *49*, 1985–2001.
- (5) Charleux, B.; Delaittre, G.; Rieger, J.; D'Agosto, F. Polymerization-Induced Self-Assembly: From Soluble Macromolecules to Block Copolymer Nano-Objects in One Step. *Macromolecules* **2012**, *45*, *6753*–*6765*.
- (6) Wan, W. M.; Hong, C. Y.; Pan, C. Y. One-Pot Synthesis of Nanomaterials via RAFT Polymerization Induced Self-Assembly and Morphology Transition. *Chem. Commun.* **2009**, *39*, 5883–5885.
- (7) Figg, C. A.; Carmean, R. N.; Bentz, K. C.; Mukherjee, S.; Savin, D. A.; Sumerlin, B. S. Tuning Hydrophobicity To Program Block Copolymer Assemblies from the Inside Out. *Macromolecules* **2017**, *50*, 935–943.
- (8) Rho, J. Y.; Scheutz, G. M.; Häkkinen, S.; Garrison, J. B.; Song, Q.; Yang, J.; Richardson, R.; Perrier, S.; Sumerlin, B. S. In Situ Monitoring of PISA Morphologies. *Polym. Chem.* **2021**, *12*, 3947–3952
- (9) Touve, M. A.; Figg, C. A.; Wright, D. B.; Park, C.; Cantlon, J.; Sumerlin, B. S.; Gianneschi, N. C. Polymerization-Induced Self-Assembly of Micelles Observed by Liquid Cell Transmission Electron Microscopy. ACS Cent. Sci. 2018, 4, 543–547.
- (10) Scheutz, G. M.; Touve, M. A.; Carlini, A. S.; Garrison, J. B.; Gnanasekaran, K.; Sumerlin, B. S.; Gianneschi, N. C. Probing Thermoresponsive Polymerization-Induced Self-Assembly with Variable-Temperature Liquid-Cell Transmission Electron Microscopy. *Matter* 2021, 4, 722–736.
- (11) Parkatzidis, K.; Truong, N. P.; Rolland, M.; Lutz-Bueno, V.; Pilkington, E. H.; Mezzenga, R.; Anastasaki, A. Transformer-Induced Metamorphosis of Polymeric Nanoparticle Shape at Room Temperature. *Angew. Chem.* **2022**, *134*, No. e202113424.
- (12) Karayianni, M.; Pispas, S. Block Copolymer Solution Self-Assembly: Recent Advances, Emerging Trends, and Applications. *J. Polym. Sci.* **2021**, *59*, 1874–1898.
- (13) Lovett, J. R.; Warren, N. J.; Ratcliffe, L. P. D.; Kocik, M. K.; Armes, S. P. PH-Responsive Non-Ionic Diblock Copolymers: Ionization of Carboxylic Acid End-Groups Induces an Order-Order Morphological Transition. *Angew. Chem., Int. Ed.* **2015**, *54*, 1279–1283
- (14) Zhang, L.; Yu, K.; Eisenberg, A. Ion-Induced Morphological Changes in "Crew-Cut" Aggregates of Amphiphilic Block Copolymers. *Science* **1996**, *272*, 1777–1779.
- (15) Ratcliffe, L. P. D.; Derry, M. J.; Ianiro, A.; Tuinier, R.; Armes, S. P. A Single Thermoresponsive Diblock Copolymer Can Form Spheres, Worms or Vesicles in Aqueous Solution. *Angew. Chem., Int. Ed.* **2019**, *58*, 18964–18970.
- (16) Yu, Y.; Zhang, L.; Eisenberg, A. Morphogenic Effect of Solvent on Crew-Cut Aggregates of Apmphiphilic Diblock Copolymers. *Macromolecules* 1998, 31, 1144–1154.
- (17) Chen, M.; Li, J. W.; Zhang, W. J.; Hong, C. Y.; Pan, C. Y. PH-and Reductant-Responsive Polymeric Vesicles with Robust Membrane-Cross-Linked Structures: In Situ Cross-Linking in Polymerization-Induced Self-Assembly. *Macromolecules* **2019**, 52, 1140–1149.
- (18) Zhang, J.; Farias-Mancilla, B.; Kulai, I.; Hoeppener, S.; Lonetti, B.; Prévost, S.; Ulbrich, J.; Destarac, M.; Colombani, O.; Schubert, U. S.; Guerrero-Sanchez, C.; Harrisson, S. Effect of Hydrophilic Monomer Distribution on Self-Assembly of a PH-Responsive Copolymer: Spheres, Worms and Vesicles from a Single Copolymer Composition. *Angew. Chem., Int. Ed.* **2021**, *60*, 4925–4930.
- (19) Tan, J.; Zhang, X.; Liu, D.; Bai, Y.; Huang, C.; Li, X.; Zhang, L. Facile Preparation of CO2-Responsive Polymer Nano-Objects via Aqueous Photoinitiated Polymerization-Induced Self-Assembly (Photo-PISA). *Macromol. Rapid Commun.* **2017**, 38, 1600508.
- (20) Wen, S. P.; Fielding, L. A. Pyridine-Functional Diblock Copolymer Nanoparticles Synthesized via RAFT-Mediated Polymer-

- ization-Induced Self-Assembly: Effect of Solution PH. Soft Matter 2022, 18, 1385–1394.
- (21) Xu, X. F.; Pan, C. Y.; Zhang, W. J.; Hong, C. Y. Polymerization-Induced Self-Assembly Generating Vesicles with Adjustable PH-Responsive Release Performance. *Macromolecules* **2019**, *52*, 1965–1975.
- (22) Audureau, N.; Coumes, F.; Guigner, J. M.; Guibert, C.; Stoffelbach, F.; Rieger, J. Dual Thermo- and PH-Responsive N-Cyanomethylacrylamide-Based Nano-Objects Prepared by RAFT-Mediated Aqueous Polymerization-Induced Self-Assembly. *Macromolecules* **2022**, *55*, 10993–11005.
- (23) Biais, P.; Engel, M.; Colombani, O.; Nicolai, T.; Stoffelbach, F.; Rieger, J. Thermoresponsive Dynamic BAB Block Copolymer Networks Synthesized by Aqueous PISA in One-Pot. *Polym. Chem.* **2021**, *12*, 1040–1049.
- (24) Chen, S.; Chang, X.; Sun, P.; Zhang, W. Versatile Multi-compartment Nanoparticles Constructed with Two Thermo-Responsive, PH-Responsive and Hydrolytic Diblock Copolymers. *Polym. Chem.* **2017**, *8*, 5593–5602.
- (25) Wang, X.; Zhou, J.; Lv, X.; Zhang, B.; An, Z. Temperature-Induced Morphological Transitions of Poly(Dimethylacrylamide)-Poly(Diacetone Acrylamide) Block Copolymer Lamellae Synthesized via Aqueous Polymerization-Induced Self-Assembly. *Macromolecules* 2017, 50, 7222–7232.
- (26) Derry, M. J.; Mykhaylyk, O. O.; Armes, S. P. A Vesicle-to-Worm Transition Provides a New High-Temperature Oil Thickening Mechanism. *Angew. Chem., Int. Ed.* **2017**, *56*, 1746–1750.
- (27) Beattie, D. L.; Mykhaylyk, O. O.; Ryan, A. J.; Armes, S. P. Rational Synthesis of Novel Biocompatible Thermoresponsive Block Copolymer Worm Gels. *Soft Matter* **2021**, *17*, 5602–5612.
- (28) Cornel, E. J.; O'Hora, P. S.; Smith, T.; Growney, D. J.; Mykhaylyk, O. O.; Armes, S. P. SAXS Studies of the Thermally-Induced Fusion of Diblock Copolymer Spheres: Formation of Hybrid Nanoparticles of Intermediate Size and Shape. *Chem. Sci.* **2020**, *11*, 4312–4321
- (29) Li, Y.; Busatto, N.; Roth, P. J. Perfluorophenyl Azides: Photo, Staudinger, and Multicomponent Postpolymerization Reactions on Homopolymers and PISA-Made Nanoparticles. *Macromolecules* **2021**, *54*, 3101–3111.
- (30) Zhang, W. J.; Hong, C. Y.; Pan, C. Y. Artificially Smart Vesicles with Superior Structural Stability: Fabrication, Characterizations, and Transmembrane Traffic. ACS Appl. Mater. Interfaces 2017, 9, 15086–15095
- (31) Boyer, C.; Liu, J.; Wong, L.; Tippett, M.; Bulmus, V.; Davis, T. P. Stability and Utility of Pyridyl Disulfide Functionality in RAFT and Conventional Radical Polymerizations. *J. Polym. Sci., Part A: Polym. Chem.* **2008**, 46, 7207–7224.
- (32) Xu, S.; Zhang, T.; Kuchel, R. P.; Yeow, J.; Boyer, C. Gradient Polymerization—Induced Self-Assembly: A One-Step Approach. *Macromol. Rapid Commun.* **2020**, *41*, 1900493.
- (33) Blanazs, A.; Madsen, J.; Battaglia, G.; Ryan, A. J.; Armes, S. P. Mechanistic Insights for Block Copolymer Morphologies: How Do Worms Form Vesicles? *J. Am. Chem. Soc.* **2011**, *133*, 16581–16587.
- (34) Figg, C. A.; Simula, A.; Gebre, K. A.; Tucker, B. S.; Haddleton, D. M.; Sumerlin, B. S. Polymerization-Induced Thermal Self-Assembly (PITSA). *Chem. Sci.* **2015**, *6*, 1230–1236.
- (35) Mukherjee, S.; Hill, M. R.; Sumerlin, B. S. Self-Healing Hydrogels Containing Reversible Oxime Crosslinks. *Soft Matter* **2015**, *11*, *6*152–*6*161.
- (36) Scheutz, G. M.; Bowman, J. I.; Mondal, S.; Rho, J. Y.; Garrison, J. B.; Korpanty, J.; Gianneschi, N. C.; Sumerlin, B. S. Gradient Copolymer Synthesis through Self-Assembly. *ACS Macro Lett.* **2023**, 12, 454–461.